Published in final edited form as:
J Immunol. 2013 November 1; 191(9): 4804–4817. doi:10.4049/jimmunol.1301307.

Fut3-dependent synthesis of sLe^a on CD44v6 mediates PMN detachment from intestinal epithelium during transepithelial migration

Jennifer C. Brazil[*], **Renpeng Liu**[†], **Ronen Sumagin**[‡], **Keli N. Kolegraff**[‡], **Asma Nusrat**[‡], **Richard D. Cummings**[†], **Charles A. Parkos**[‡], and **Nancy A. Louis**[*]

[*]Division of Neonatal-Perinatal Medicine, Emory University School of Medicine, Atlanta, Georgia

[†]Division of Biochemistry, Emory University School of Medicine, Atlanta, Georgia

[‡]Epithelial Pathobiology Unit, Department of Pathology and Laboratory Medicine, Emory University School of Medicine, Atlanta, Georgia

Abstract

PMN migration across the intestinal epithelium closely parallels disease symptoms in patients with inflammatory bowel disease (IBD). PMN transepithelial migration (TEM) is a multistep process that terminates with PMN detachment from the apical epithelium into the lumen. Using a unique mAb (GM35), we have previously demonstrated that engagement of the V6 variant of CD44 (CD44v6) blocks both PMN detachment and cleavage of CD44v6. Here, we report that PMN binding to CD44v6 is mediated by protein-specific O-glycosylation with sialyl Lewis A (sLe^a). Analyses of glycosyltransferase expression identified fucosyltransferase 3 (Fut3) as the key enzyme driving sLe^a biosynthesis in human intestinal epithelial cells (IECs). Fut3 transfection of sLe^a-deficient IECs resulted in robust expression of sLe^a. However, this glycan was not expressed on CD44v6 in these transfected IECs, and therefore engagement of sLe^a had no effect on PMN TEM across these cells. Analyses of sLe^a in human colonic mucosa revealed minimal expression in noninflamed areas, with striking upregulation under colitic conditions that correlated with increased expression of CD44v6. Importantly, intraluminal administration of mAb GM35 blocked PMN TEM and attenuated associated increases in intestinal permeability in a murine intestinal model of inflammation. These findings identify a unique role for protein-specific O-glycosylation in regulating PMN-epithelial interactions at the luminal surface of the intestine.

Introduction

The migration of polymorphonuclear leukocytes (PMN) out of the circulation across both endothelial and epithelial cell barriers is critical to the host inflammatory response to infection and injury. When dysregulated, the influx and accumulation of PMN in intestinal crypts is also a hallmark of the symptomatic phase of many intestinal inflammatory processes, including Crohn's disease and ulcerative colitis (UC) (1, 2). Considerable progress has been made in understanding the steps involved in PMN trafficking across

Corresponding author: Dr. Nancy A. Louis, M.D., Division of Neonatal-Perinatal Medicine, Emory University School of Medicine, 2015 Uppergate Drive, Suite 320, Atlanta, GA 30322, Phone: (404) 727-3360; Fax (404) 727-3236, nlouis@emory.edu.

vascular endothelium (3-5) and intestinal epithelium (6-9). Additionally, the mechanisms governing late events in PMN transmigration across mucosa, including PMN detachment and release from the apical surface of epithelia into the lumen, while incompletely characterized, have become a recent focus for investigation. It has been previously reported that epithelial intracellular adhesion molecule 1 (ICAM-1) is expressed apically and acts as a PMN retention ligand under inflammatory conditions (8). In addition PMN Fc receptor interactions with apical epithelial proteins have also been implicated in PMN-epithelial retention (10), and it has previously been reported that decay-accelerating factor (DAF) functions as an anti-adhesive epithelial glycoprotein that regulates PMN detachment from the epithelium (11). As described further below, we recently reported that a CD44 isoform containing variant exon 6 (CD44v6) regulates detachment of migrating PMN from the apical epithelial surface into the intestinal lumen (12).

CD44 represents a heterogeneous, though monogenic (13) group of cell surface glycoproteins implicated in multiple cellular functions including, but not limited to, cell-cell adhesion (14), cell migration (15), and cell matrix adhesion (16). The amino terminal globular domain of CD44 proteins is separated from the transmembrane domain by a short stem structure that contains putative proteolytic cleavage sites (17). This stem structure can be extended by the insertion of CD44 variant exons, giving rise to the large variant isoforms of CD44, the expression of which is restricted to rapidly dividing cells including epithelial cells, activated lymphocytes and some tumor cells (18-20). The extracellular domains of CD44 variant proteins are known to contain motifs for post-translational modifications including numerous sites for N- and O-linked glycosylation (21). CD44 protein diversity is therefore generated both by alternative splicing of variant exon-encoded gene products in the membrane proximal extracellular domain region (22), and by cell-type specific differences in glycosylation (23, 24). One such variant is CD44v6 for which we developed a specific mAb (GM35). Using this mAb we recently described a role for shedding of the extracellular domain (ECD) of CD44v6 in PMN detachment from the surface of the apical epithelium (12). Despite the highly glycosylated nature of CD44 variant isoforms, the role of specific glycosylation motifs in the function of these important proteins has yet to be characterized.

In this study, we investigated factors regulating PMN release from the apical epithelium. We show that, during inflammation, PMN detachment from the apical surface of the intestinal epithelium is regulated by glycan epitopes present on CD44v6. We demonstrate that the functionally-inhibitory effects of the O-glycan-binding mAb GM35 are meditated through sialic acid-dependent binding to sLe^a specifically expressed on CD44v6, and that sLe^a synthesis is Fut3-dependent. Analyses of sLe^a and CD44v6 in human colonic mucosa revealed expression that was restricted to regions of active inflammation. Inhibitory effects of mAb GM35 on PMN TEM were confirmed in an in vivo model of intestinal inflammation, where blockade of PMN TEM also prevented PMN-dependent increases in intestinal permeability.

Materials and Methods

Cell Culture

Cultures of T84 (25), HT29 (26), Caco2 (11) and SKCO15 (27) IECs were grown as previously described.

Antibodies and Reagents

Monoclonal anti-CD44v6 antibody was purchased from R&D Systems (Minneapolis, MN). Monoclonal anti-desmoglein mAb was purchased from Santa Cruz Biotechnology Inc. (Santa Cruz, CA). Monoclonal anti-sLe^a antibody (NS19-9) was purchased from Dako (Carpinteria, CA). Anti-sLe^x mAb (CD15s) was purchased from BD (Franklin Lakes, NJ). The anti-sLe^c mAb (Dupan-2) was purchased from Glycotech Corporation (Rockville, MD). Anti-Fut3 mAb was purchased from Abcam (Cambridge, MA). mAb GM35 was isolated as described previously (12). The anti-CD11b/CD18 mAb CBRM1/29 has been described elsewhere (28). Antibodies against Siglec-5, Siglec-9 and Siglec-14 were purchased from Abcam (Cambridge, MA) and BD bioscience (San Jose, CA). Protein G Sepharose beads were purchased from GE Healthcare Life Sciences (Pittsburgh, PA). Zenon ® Alexa Fluor ® 488 Mouse IgG_1, 568 Mouse IgG_1 and 568 Mouse IgG_{2b} labeling kits were purchased from Invitrogen Corporation (Carlsbad, CA). Bovine serum albumin, chemotactic peptide N-Formyl-L-methionyl-L-leucyl-L-phenylalanine (fMLF), 2,2′-azino-bis(3-ethylbenzthiazoline-6-sulphonic acid (ABTS), 2-acetamido-2-deoxy-α-D-galactopyranoside (Benzyl-Gal-NAc), iodecetamide, guanidinium chloride, streptavidin, dithiothreitol and neuraminidase from *Arthrobacter ureafaciens* were purchased from Sigma-Aldrich (St. Louis, MO). Tunicamycin was purchased from Calbiochem (La Jolla, CA). Kifunensine was purchased from EMD Chemicals (Newark NJ). N-Glycosidase F/PNGase-F was purchased from New England Biolabs (Ipswich, MA). Full length CD44 in a pCMv6 entry vector plasmid, CD44 specific short hairpin RNA (shRNA) constructs and a Scr construct plasmid in pGFP-V-RS vectors and Fut3 and Scr siRNA duplexes were purchased from Origene (Rockville, MD). Human CD44var6 (CD44v6) instant ELISA kits were purchased from Bender Medsystems (Vienna, Austria). SYBR green superrmix was purchased from Biorad (Hercules, CA).

Treatment of human IECs with glycosylation inhibitors

To block N-glycosylation, T84 or HT29 IECs cells were grown in the presence or absence of tunicamycin at 5μg/ml in complete medium for 24h at 37°C. To block O-glycan extension, cells were incubated with 5mM benzyl GalNAc in complete media for 24-48 hours at 37°C. For removal of sialic acid, T84 and HT29 IEC protein lysates were treated with neuraminidase overnight at 4°C according to manufacturers instructions.

Glycan Microarray Assay

Antibodies were submitted for glycan binding analysis to the Consortium for Functional Glycomics (CFG) (http://www.functionalglycomics.org) - GM35 (cfg_rRequest_2785, pa_v5), at 0.1μg/ml and the anti-sLe^a antibody NS19-9 (cfg_rRequest_1982, pa_v41), and the anti-sLe^c antibody Dupan-2 (cfg_rRequest_2614, pa_v51), at 10μg/ml. These glycan

microarrays contain up to 611 individual structures, representing a library of known natural and synthetic mammalian glycans, in replicates of 6. Binding of antibodies to specific glycan epitopes was detected using fluorescently labeled secondary antibodies. An RFU of greater than or equal to 500 was set as a threshold indicative of positive binding.

PMN isolation

PMN were isolated from whole blood obtained from normal human volunteers, with approval from the Emory University Institutional Review Board on human subjects, by using a previously described density gradient centrifugation technique (29). PMN were re-suspended in HBSS with 10mM Hepes, pH7.4, and without Ca^{2+} or Mg^{2+} at a concentration of 5×10^7 cells/ml. Neutrophils isolated in this way were 97% pure and >95% viable and were used for transmigration within 2 hours of blood draw.

PMN Transmigration Assay

For transmigration experiments, IECs were grown on collagen-coated, permeable 0.33-cm^2 polycarbonate filters (5μm pore size; Costar Corp.) as described previously (9, 25, 30). All epithelial migration experiments were performed in the physiologically relevant basolateral-to-apical direction (i.e. inverted monolayers), in the presence of a chemotactic gradient of 100nM fMLF. For migration experiments, 1×10^6 PMN were added to the upper chambers of transwell inserts and migration was measured at 37°C for indicated times in the presence of 10μg/ml apically applied GM35, NS19-9, Dupan-2 or isotype control mAb. For analysis of effects of sialic acid-binding immunoglobulin-type lectins (Siglecs) on the GM35 mediated blockade of PMN TEM, PMN were pre-incubated with 10μg/ml Abs against Siglec-5, Siglec-9 and Siglec-14 for 20 minutes before the initiation of PMN TEM. Transmigrated PMN were quantified by assaying for the PMN azurophilic marker myeloperoxidase (MPO) as described previously (31). PMNs, which migrated through tight junctions yet remained adherent to the apical surface of the T84 IEC monolayer after basolateral-to-apical migration, were quantified using a previously described procedure (10). Briefly, after completion of transmigration, T84 monolayers were removed and transferred to new tissue culture plates containing 1ml HBSS/well. Plates were spun for 5 min in order to release PMN that had migrated through junctions yet remained adherent to the apical surface (50g, 4°C). Detached PMN were quantified by MPO assay as above.

Enzyme Linked Immunoadsorbent Assay (ELISA) detection of soluble CD44v6

PMN were isolated and stimulated to migrate across confluent T84 monolayers in the physiologically relevant basolateral to apical direction in the presence or absence of apically applied NS19-9 (10μg/ml), as described above. Samples from the apical reservoir were removed at 0, 5, 15, 30, 45 and 60 minutes and assessed for levels of soluble CD44v6 (sCD44v6) using a CD44v6 ELISA kit according to manufacturer's instructions. A standard curve was prepared from six standard dilutions of sCD44v6 and levels of sCD44v6 in experimental samples and standards were measured at 450nm.

Immunoblotting and Immunprecipitation

Cell lysates for immunoblotting were prepared with the following lysis buffer (20mM Tris pH 7.5, 150mM NaCl, 1mM EDTA, 1% TX-100, 1mM Na_3VO_4, and 1mM PMSF) supplemented with 10% mammalian tissue protease inhibitor cocktail (Sigma-Aldrich, St. Louis, MO). For immunprecipitation experiments, pre-cleared cell lysates were incubated with 2μg of relevant mAb for 4h at 4°C, followed by incubation with protein G-Sepharose beads overnight at 4°C. Washed immunoprecipitates and regular cell lysates were boiled in SDS-PAGE sample buffer under reducing conditions, and then subjected to SDS-PAGE followed by transfer to PVDF under standard conditions. Membranes were blocked with 4% milk and incubated with 1μg/ml of the indicated mAb. Primary antibodies were detected using appropriate HRP-linked secondary antibodies (Jackson Immunoresearch laboratories, West Grove, PA). Murine small intestine and colonic mucosal epithelial lysates were prepared after the serosa and external longitudinal layer of the muscularis propria were stripped away. Isolated mucosal sheets were solubilized in SDS sample buffer and analyzed for protein expression by immunoblot using indicated antibodies. Primary antibody binding was detected with relevant HRP conjugated secondary antibody (CD44v6) or with HRP labeled streptavidin for biotinylated GM35.

Isolation of glycoconjugates

Human IECs (T84, SKCO15 and Caco2) were processed first by adding 8M Guanidinium HCL in 0.2 M Tris (pH 8.2). Proteins were then denatured by dithiothreitol (DTT) and alkylated by iodoacetamide. Denatured samples were dialyzed against water overnight before lyophilization was performed. Lyophilized proteins were subsequently digested with trypsin in 50mM phosphate buffer (pH 8.2) to generate glycopeptides that were susceptible to digestion with N-glycosidase (PNGase F). Following PNGase F digestion, released N-glycans were obtained from the run-through of C-18 cartridges and collected by elution followed by subsequent application to a Carbograph cartridge. Remaining peptides and glycopeptides containing the O-glycans were obtained by elution with 80% and 100% methanol from the C-18 cartridge. O-linked glycans were released by sodium hydroxide mediated reductive β-elimination (50mM NaOH, 1M $NaBH_4$) at 45°C for 16h. Released O-glycans were obtained in the run-through of C-18 cartridges and collected by elution from a subsequent application to a Carbograph cartridge.

Permethylation of glycans

N-and O-glycans were permethylated by sodium hydroxide and iodomethane in DMSO to allow for further structural analysis. Reactions were quenched by ddH_2O after 1 hour and the samples were extracted by chloroform before further washing with ddH_2O. The chloroform fraction was gently dried by nitrogen gas and re-dissolved in a 1:1 mix of Methanol and ddH_2O. The samples were loaded onto a C-18 cartridge and eluted stepwise with ddH_2O and 15%, 35%, 50% and 75% aqueous acetonitrile. Permethylated glycans were usually present in the 35%, 50% and 75% acetonitrile fractions.

Mass spectrometry analysis of glycans

An Ultraflex-II TOF/TOF system (Bruker Daltonics, Fremont, CA) was used for MALDI-TOF mass spectrometric analysis. Reflective positive modes were used as indicated in the figures. The 2,5-dihydroxybenzoic acid (5mg/ml in 50% acetonitrile, 0.1% TFA) was freshly prepared to use as the matrix. 0.5μl matrix solution was spotted onto an Anchorchip target plate (200μm or 400μm) and air-dried before 0.5μl sample solution was applied and also allowed to air dry. The MS/MS data were acquired in positive reflector mode using an Applied Biosystem MALDI-TOF/TOF 4800 plus (Applied Biosystems, Foster City, CA). The collision energy was set to 2kV, and argon was used as collision gas. Data were acquired using the 4000 Series Explorer Instrument Control Software and were processed using Data Explorer MS processing software (Applied Biosystems, Foster City, CA). MS/MS spectra were assigned and annotated with the help of the GlycoWorkbench tool from EuroCarbDB (www.eurocarbdb.org).

Flow Cytometry and Immunostaining

PMN were isolated as described above and incubated with GM35 (10μg/ml), NS19-9 (10μg/ml), anti-sLe^x mAb (10μg/ml), anti-CD44v6 mAb (10μg/ml) or the anti-CD11b/CD18 mAb CBRM1/29 (10μg/ml). Following washing, PMN were incubated with a FITC labeled secondary antibody, fixed in 2% PFA, and analyzed by flow cytometry. Flow cytometric analysis was carried out using a FACScan (Becton Dickinson, Franklin Lakes, NJ) equipped with an argon ion laser tuned at a 488 nm wavelength.

Immunofluorescent labeling of IECs was achieved as follows. Non-permeabilized T84 monolayers were fixed using absolute Ethanol and subsequently blocked with 3% bovine serum albumin. Monolayers were then incubated with Zenon Alexa Fluor® labeled primary antibodies (10μg/ml) or with primary antibodies and fluorescently labeled secondary antibodies. Following antibody incubations, monolayers were mounted in ProLong anti-fading embedding solution (Invitrogen Life Technologies, San Diego, CA). Images shown were representative of at least three experiments with multiple images taken per monolayer.

For human tissue staining, frozen sections (6μm) of discarded resection specimen colonic mucosa from patients with ulcerative colitis were obtained. Inflamed and non-inflamed sections of discarded tissue were characterized based on observed extent of disease activity. Tissue was fixed in absolute ethanol, non-specific protein binding was blocked with 3% BSA and tissue sections were incubated with primary antibodies, washed in HBSS$^+$, and subsequently labeled with appropriate secondary antibodies or with Zenon Alexa Fluor labeled primary antibodies (10μg/ml). Nuclei were stained with TO-PRO-3 iodide (1:1000 × 5min, room temperature, Invitrogen Life Technologies, San Diego, CA). For immunohistochemistry tissue sections were incubated with GM35 at 10μg/ml followed by haemotoxylin and eosin staining to detect primary antibody binding. All procedures on discarded human tissue were carried out under Emory IRB approval. All images were captured using an LSM 510 confocal microscope (Carl Zeiss Microimaging, Thornwood, NY) with pan-Neofluor 40×/1.3 oil objective using software supplied by the vendor.

Transcriptional analysis

Human IECs were lysed in TRIzol (Invitrogen Life Technologies, San Diego, CA), then subjected to phenol-chloroform extraction according to the manufacturer's protocol as described previously (32). RNA was digested with DNase I (Ambion, Austin, TX) to remove contamination with genomic DNA, and then cDNA was synthesized by reverse transcription using oligo(dT12-18) primers and superscript II reverse transcriptase (Invitrogen, Grand Island, NY). Real-time PCR was performed using a MyIQ real-time PCR machine and SYBR Green supermix (BioRad, Hercules, CA). Data were analyzed by the $\Delta\Delta C_t$ threshold cycle method and normalized to the housekeeping gene GAPDH as previously described (33).

Murine in vivo PMN trafficking assays

Male wild type (WT) C57BL/6J mice (Jackson Laboratories) were maintained under specific pathogen-free conditions at Emory Division of Animal Resources facilities. Following overnight fasting, animals aged between 11-15 weeks were anesthetized by subcutaneous intramuscular injection of a mixture of 100mg/kg ketamine and 5mg/kg xylazine. Next, a midline abdominal incision was made and a 4cm loop of small intestine was exteriorized and ligated at both proximal and distal ends (Fig 7B). For PMN migration experiments, isolated intestinal loops were injected with 100μM fMLF or 500ng of the PMN chemoattractant CXCL1 (KC), +/− 50μg indicated mAb, in 200μl $HBSS^+$ followed by loop reinsertion into the peritoneal cavity. The abdomen was then sutured closed and the animal was monitored for a 90-minute incubation. Mice were then euthanized via rapid cervical dislocation, and the abdomen reopened. Intestinal loops were isolated and lavaged twice with $HBSS^+$. The number of PMN reaching the intestinal lumen was quantitated based on cytospin analysis and Diff-Quik staining of the lavage fluid (Dade Behring, Newark, DE).

For dextran flux assays, isolated intestinal loops were injected with 100μM fMLF and indicated antibodies (50μg GM35 or IgG control mAb) before re-insertion into the anesthetized mice for a 60-minute incubation. Following the initial incubation FITC-dextran (10kDa, 1mg/ml in 200μl saline) was injected into the intestinal loop and mice were monitored for an additional 30 minutes. Passage of dextran out of the intestine into the vasculature was assessed through the measurement of fluorescence in peripheral blood (obtained through cardiac puncture) using the Fluostar Galaxy plate reader (BMG LabTech, Germany). Following cardiac puncture, mice were euthanized via rapid cervical dislocation. To assess the role of PMN influx in the observed changes in barrier permeability following introduction of fMLF to the lumen of the murine small intestine, PMN were depleted as previously described (34). Briefly, anti-Ly6G antibody, (200μg/mouse) was injected into the intraperitoneal cavity of mice 24 hours before exteriorization of the small intestine loop and dextran flux assay, as described above. All animal protocols were reviewed and approved by the Institutional Animal Care and Use Committee of Emory University.

Data analysis

Statistical differences were determined by 2-factor ANOVA using PRISM 5 for Mac OSX version 5.0a 1992-1998, Graphpad software, Inc. Values are expressed as the mean and SE from at least three separate experiments.

Results

Closely regulated PMN translocation into the intestinal lumen is a crucial part of a successful host response to infection and injury. However, dysregulation of PMN influx into the intestinal tissues is also indicative of IBD. In studies to characterize surface molecules that regulate PMN TEM, we generated a unique mAb (GM35) that blocks PMN trafficking into the intestinal lumen through binding to an epitope on the apically expressed epithelial protein CD44v6 (12).

GM35 binds the O-linked glycan sLe^a in a sialic acid-dependent fashion

CD44v6 is a high molecular weight member of the widely distributed type I transmembrane CD44 family of glycoproteins. Previous reports have indicated that the extracellular domains of CD44 variant proteins, including CD44v6, are extensively post-translationally modified to contain N- and O-glycans (13, 21). To determine if the functional effects of CD44v6 engagement were mediated specifically through glycan binding, T84 and HT29 IECs, previously shown to express the GM35 epitope, were exposed to glycosylation inhibitors prior to cell lysis and analysis of antigen expression by immunoblot. Pre-treatment of these IECs with the inhibitor of N-glycosylation, tunicamycin (Fig. 1A), or the inhibitor of complex-type N-glycan formation, kifunensine (data not shown), had no effect on expression of the GM35-binding epitope on CD44v6. In contrast, treatment with Benzyl-GalNAc, a small, synthetic sugar analogue that competitively inhibits the terminal glycosylation of core 1-O-glycans and subsequent downstream formation of core 2-O-glycans (35), significantly reduced the level of epitope detection by GM35 in T84 and HT29 IECs (Fig. 1B). These findings are consistent with prior reports indicating that the glycans on the extracellular variant exon-encoded regions of CD44 proteins are predominantly O-linked (21).

To both confirm the specificity of GM35 for a carbohydrate ligand and further characterize the glycoepitope recognized by this mAb, the affinity of GM35 binding to specific glycan determinants was analyzed on a glycan microarray developed by the Consortium for Functional Glycomics (CFG). These glycan arrays contain immobilized glycans, representing a variety of known glycan structures presented on both N- and O-glycan backbones, as described under *Methods*. The results show that GM35 binds strongly to each of three glycans containing the tetrasaccharide determinant Neu5Acα2-3Galβ1-3(Fucα1-4)GlcNAc-R (Fig. 1C). This glycan determinant is composed of four monosaccharides, N-acetylneuraminic acid (Neu5Ac, sialic acid), Galactose (Gal), Fucose (Fuc) and N-acetylglucosamine (GlcNAc), and represents the human blood group antigen Sialyl Lewis A (sLe^a). Further analysis revealed almost equivalent binding of GM35 to sLe^a as a component of the extended structures sLe^a-sLe^x (Glycan No.1) and sLe^a-sLe^a (Glycan No. 2), with weaker binding to the sLe^a tetrasaccharide alone (Glycan No. 3) (Fig. 1C). In addition to these strong interactions with sLe^a-containing glycans, microarray analysis also revealed weaker binding of GM35 to a variant form of sLe^a containing N-glycolyneuraminic acid (Neu5Gc), a derivative of N-acetylneuraminic acid not normally synthesized in humans, but which has been reported to be present in certain cancers (36). It was also interesting to note that GM35 recognized sLe^a with both high affinity and

specificity, in that GM35 showed no reactivity to glycans on the array terminating in its structural isomer, sialyl Lewis X (sLe^x) (Neu5Acα2-3Galβ1-4(Fucα1-3)GlcNAc) (Glycan No.9, Fig. 1C).

Glycan binding analysis also revealed lower affinity recognition by GM35 of the non-fucosylated sLe^a precursor, so-called Sialyl Lewis C (sLe^c) (Neu5Acα2-3Galβ1-3-GlcNAc) (Fig. 1C, Glycans 4,5,7,8). mAbs against sLe^a and sLe^c are commercially available with anti-sLe^a mAbs commonly used to screen for tumors of intestinal, hepatic and pancreatic origin (37). Therefore, as a positive control for glycan recognition specificity, glycan microarray analyses of the anti-sLe^a mAb NS19-9 (38), and the anti-sLe^c mAb Dupan-2 (39) were performed. Results confirmed the specific binding of mAb NS19-9 to the tetrasaccharide sLe^a (Supplemental Fig. 1A). Furthermore, the three sLe^a-containing glycans recognized with the highest binding by GM35 were identical to those recognized most avidly by mAb NS19-9. In addition glycan array analyses revealed that mAb Dupan-2 bound specifically to two sLe^c variant glycans (Supplemental Fig. 1B) which contained the three sLe^c constituent sugars in the same conformation as the sLe^c glycan structures recognized by GM35 (Fig. 1C).

While sLe^a in its entirety is common to the glycans binding GM35 with highest affinity, all the glycans, even those recognized by GM35 with lower affinity, contain a terminal sialic acid residue linked to galactose by an α-2-3 linkage. To further characterize the GM35 carbohydrate binding interaction, the role of the terminal sugar residue Neu5Ac was examined. Removal of Neu5Ac from IEC protein lysates by neuraminidase treatment resulted in a complete ablation of GM35 binding, suggesting a crucial role for this sugar moiety in the binding of GM35 to its primary target sLe^a (Fig. 1D). Having identified the role of (GM35 binding) sialylated epithelial epitopes in PMN TEM, we next wanted to investigate candidates for the PMN sialic acid binding receptor responsible for the GM35-mediated blockade of PMN TEM (12). Therefore, the potential contributions of the known PMN-expressed sialic acid-binding immunoglobulin-type lectins (Siglecs −5,−9,−14) (40) to the GM35-mediated block of PMN TEM was assessed. Pre-incubation of PMN with functionally active antibodies against Siglec 5, 9 and 14 (41, 42) had no significant effect on the GM35-mediated block in PMN TEM (Supplemental Fig. 1C). These findings suggest that previously reported PMN-expressed Siglecs are unlikely to be the counter ligand(s) for the sialylated binding epitope recognized by GM35 on intestinal epithelium.

Anti-sLe^a mAb NS19-9 but not anti-sLe^c mAb Dupan-2 inhibits PMN TEM

We have previously demonstrated that the GM35 binding epitope is not expressed on the surface of PMN (12), and thus its effects on PMN TEM must be mediated through specific interactions with the epithelium. Furthermore, immunoblotting analyses confirmed variations in IEC line expression of sLe^a, as detected by mAb NS19-9. A large sLe^a-positive glycoprotein of a similar size to the protein recognized by GM35 (12) was detected by mAb NS19-9 in both T84 and HT29 IECs, but not in SKCO15 or Caco2 cells (Fig. 2A). Consistent with these findings, neither NS19-9 nor GM35 had any effect on PMN TEM across Caco2 monolayers (data not shown). This cell-specific pattern of expression for sLe^a is consistent with our prior observations for the GM35 antigen (12). In contrast, sLe^c was

expressed by T84, HT29, and SKCO15, but not by Caco2 IECs (Fig. 2B). Interestingly, while T84 and HT29 but not Caco2 cells are known to independently express CD44v6 and sLe^a (43-45), the relationship between these two entities has not been previously studied.

Next, we examined the functional effects of mAbs specific for either sLe^a (NS19-9) or sLe^c (Dupan-2) on PMN TEM. Apical treatment of T84 IECs with NS19-9 significantly inhibited PMN TEM, relative either to control IECs treated without Ab ($p<0.01$), or to those treated apically with a non-inhibitory IgG binding control antibody ($p<0.01$) (Fig. 2C). Furthermore, the reduction in PMN TEM was associated with a significant increase in the numbers of PMN that had crossed through tight junctions yet remained adherent to the apical surface of the epithelium (Fig. 2D). Thus, the arrest in TEM occurred at the level of detachment from the apical epithelial membrane, as we have previously reported for GM35-mediated blockade of PMN TEM (12). Analysis of the kinetics of the effects of NS19-9 revealed consistent inhibition of migration over a 3-hour time-course (Fig. 2E). Although immunofluorescent analysis of the subcellular localization of sLe^c on T84 IECs demonstrated low levels of apical expression of this carbohydrate structure (Fig. 2F), this anti-sLe^c mAb had no effect on PMN TEM across T84 IECs (Fig. 2G), indicating that the carbohydrate determinants that regulate intestinal trafficking of PMN are highly specific.

Given our prior findings that ligation of the GM35 ligand inhibits PMN TEM by blocking shedding of CD44v6, we next explored the effect of NS19-9-dependent masking of the sLe^a glycoepitope on PMN TEM-dependent cleavage of CD44v6. ELISA-based detection of soluble CD44v6 ECD in the apical supernatants from T84 IECs following PMN TEM (Fig. 2H), confirmed our previous findings that significant levels of CD44v6 were released from T84 IECs between 30 and 60 minutes of PMN TEM (12). Furthermore, binding of NS19-9 to epithelial sLe^a blocked the release of CD44v6 (Fig. 2I). In contrast to the effects seen when NS19-9 is present for the duration of the migration assay, addition of mAbs against sLe^a following completion of PMN migration did not prevent the detection of shed CD44v6 (Fig. 2J). These data demonstrate that NS19-9 (and GM35, data not shown) do not prevent binding of released CD44v6 to the capture or detection Abs of the ELISA, but rather that binding of mAbs to sLe^a interferes with the release of epithelial CD44v6.

NS19-9 recognizes sLe^a displayed by an O-linked glycan on CD44v6

NS19-9 was next used to confirm that the sLe^a expressed by T84 and HT29 IECs was displayed on an O-linked carbohydrate backbone. Indeed, treatment of T84 and HT29 IECs with Benzyl-GalNAc but not tunicamycin reduced recognition of the sLe^{a}carbohydrate epitope by mAb NS19-9 (Fig. 3A,B). In addition pre-treatment of IEC protein lysates with neuraminidase ablated binding of the anti-sLe^a mAb NS19-9 to its O-linked carbohydrate epitope (Fig. 3C), demonstrating that the negatively charged sialic acid residue is again critical for Ab-mediated recognition of sLe^a.

Given that GM35 was initially characterized as binding to the transmembrane glycoprotein CD44v6 (12), the relative contribution of CD44-specific-sLe^a to total detected levels of sLe^a was next assessed. shRNA-based attenuation of CD44 expression was performed in the readily-transfectable, sLe^a expressing HT29 IECs. As we have reported previously for the GM35 antigen (12), knockdown of CD44v6 protein expression in HT29 IECs by shRNA

plasmids (data not shown) also corresponded to a significant reduction in the expression of sLe^a as detected by NS19-9 (Fig. 3D).

We next employed glycomic analyses to gain a broader understanding of the global similarities and differences in glycosylation patterns across IEC lines in order to further define the structure of sLe^a-containing glycans on T84 IECs, as well as to identify candidate mechanisms for differential regulation of sLe^a synthesis. Analysis of N- and O-glycans released from T84 IECs using MALDI-TOF mass spectrometry revealed that O-glycans from T84 IECs have compositions dominated by predicted core 1 (*m/z* 1256.5 and 895.2) and core 2 structures (*m/z* 983.4, 1344.4 and 1705.6) (Fig. 3E). Also included among the predicted O-glycans are several higher molecular weight extended core 2 structures (*m/z* 1879.9, 2329.0, and 2503.1). Importantly, analysis of the O-glycan profile from T84 IECs revealed numerous sialyl Lewis moieties on these core 2 and extended core 2 structures (*m/z* 1518.6, 1879.8, 1967.8, 2141.9, 2329.0, and 2503.1). While mass spectrometry by this approach cannot distinguish between the structural isomers sLe^a and sLe^x, our biochemical analyses of the sLe^a binding mAbs GM35 and NS19-9, as well as the anti-sLe^x mAb CD15s (data not shown), make it likely that the sialyl Lewis structures detected here are sLe^a. Of note, surface glycan profiling also indicated that the sLe^c structures on T84 IECs are confined to N-glycans (Fig. 3F).

In contrast to the extensive glycosylation of T84 IECs, the O-glycans released from SKCO15 (Supplementary Fig. 2A,B) were much less complex, and Caco2 (Supplementary Fig. 2C,D) IECs had decreased structural complexity of both N- and O-glycans. Thus, in addition to differences in sLe^a expression, these IEC lines also revealed more global differences in total N- and O-glycosylation. Furthermore, there were no sialyl Lewis structures of any kind displayed by either the N- or O-glycans from SKCO15 IECs. Mass spectrometry analysis of the glycans displayed by Caco2 IECs did reveal low levels of expression of a small number of predicted sialyl Lewis structures (m/z 1519, 1880.4). However, given the lack of GM35 (12) and NS19-9 binding (Fig. 2A) to Caco2 IECs, and the positive binding of the anti-sLe^x mAb CD15s to Caco2 lysates by immunoblot (data not shown), these sialylated Lewis antigen structures detected by MALDI-TOF are most likely to be sLe^x rather than sLe^a.

To further characterize the sLe^a-containing glycans displayed by T84 IECs, MS/MS analysis of the O-glycans was performed through collision-induced-dissociation (CID), demonstrating that the six O-linked sialyl Lewis-containing glycans on T84 IECs are core-2 structures (Supplementary Fig. 3A-F). MALDI-TOF mass spectrometry analysis also revealed that the N-glycans from T84 IECs are mainly composed of high mannose-type glycans, ranging from $Man_5GlcNAc_2$ to $Man_9GlcNAc_2$ (*m/z* 1579.8, 1784.0, 1988.1, 2192.2 and 2396.3) with minor biantennnary (*m/z* 2605.6) or triantennnary (*m/z* 3590.0) complex-type structures (*m/z* 2605.6, 3590.0) (Fig. 3F). Importantly, analysis of the N-glycans from T84 IECs revealed no expression of any sialyl Lewis structures. Therefore, the combined results of immunoblot and mass spectrometry demonstrate that the sLe^a antigen in T84 IECs is found only on core 2 or extended core 2 O-glycans.

Differential expression of sLe^a corresponds to differential glycosyltransferase expression

Mass spectrometric analyses revealed global differences in the extent and complexity of glycosylation across IECs, and that sLe^a is confined to core 2 O-glycans. sLe^a synthesis is also likely to be regulated, at least in part, by enzymes directly implicated in the biosynthesis of the family of sialylated Lewis structures. Therefore, the differential expression of glycosyltransferases with potential roles in sLe^a synthesis (Fig. 4A), including fucosyl and sialyltransferases, was examined in IEC lines, which either expressed both CD44v6 and sLe^a (T84 and HT29), expressed CD44v6 but not sLe^a (SKCO15), or expressed neither CD44v6 nor sLe^a (Caco2).

Comparison of the RNA levels of specific fucosyltransferases revealed that Fut3 expression was increased ~75-fold in T84 IECs, relative to SKCO15 and Caco2 ($p < 0.01$, Fig. 4B). Although considered to be an α1-3/4 fucosyltransferase, Fut3 is predominantly known to exhibit α1-4 fucosyltransferase activity (46, 47). In addition to changes in Fut3 expression, a 7-fold increase in the expression of α1-3-Fut6 was also observed in T84 relative to Caco2 IECs ($p < 0.05$) but not relative to SKCO15 cells (Fig. 4B). However, Fut6 has previously been implicated in the generation of sLe^x but not sLe^a (46). No other significant differences were observed for the expression of the additional fucosyltransferases examined (Supplementary Fig. 4C).

The expression levels of ST3Gal sialyltransferases, which catalyze the addition of N-acetylneuraminic acid to galactose during sLe^a synthesis, were also examined. Results demonstrate the expression of α2,3-ST3Gal3, which has been shown to be important for sLe^a synthesis in other cells (46), was significantly lower in T84 cells relative to Caco2 and SKCO15 cells. Thus, another sialyltransferase such as α2,3-ST3Gal2 may be involved in sLe^a biosynthesis in T84 IECs (Fig. 4B). No other significant differences in the expression of ST3Gal sialyl transferases were observed (Supplemental Fig. 4B). Observed differences in ST3Gal3 and Fut3 gene expression were subsequently confirmed at the level of protein expression in that T84 IEC lysates revealed increases in Fut3 (Fig. 4C) and lower ST3Gal3 protein expression relative to SKCO15 and Caco-2 IECs.

Fut3 expression drives sLe^a synthesis in CD44v6 expressing cells

In order to determine whether the observed lack of Fut3 expression was truly related to the absence of sLe^a in specific IEC lines, a plasmid containing full length Fut3, which naturally has both α1,3- and α1,4-fucosyltransferase activities, was transfected into sLe^a-deficient SKCO15 cells. Indeed, transfection with Fut3 resulted in robust expression of this fucosyltransferase relative to SKCO15 cells transfected with an empty vector (Fig. 5A). In addition, overexpression of Fut3 correlated with the expression of a large glycoprotein that was detected with GM35 (Fig. 5A) and NS19-9 (not shown), suggesting that Fut3 expression can drive sLe^a biosynthesis in these IECs. To further demonstrate the importance of Fut3 synthesis for sLe^a generation in human IECs, expression of Fut3 was knocked down in HT29 IECs. Transfection with Fut3 siRNA decreased Fut3 expression and corresponded to a decrease in sLe^a expression detected by GM35 or NS19-9 (data not shown), relative to non-transfected HT29 IECs and to cells transfected with Scr siRNA (Fig. 5B).

The effects of mAb GM35 on PMN TEM across Fut3/sLe^a expressing SKCO15 IECs were next assessed. Despite successful induction of both Fut3 and sLe^a expression, mAb GM35 had no effect on PMN trafficking across sLe^a expressing SKCO15 cells (Fig. 5C). However, IF analysis of the expression of surface epitopes in these transfected IECs revealed little to no co-localization of sLe^a and CD44v6 (Fig. 5D). This suggests that while Fut3 expression does drive sLe^a synthesis in SKCO15 IECs, these cells lack other intracellular processes necessary for the posttranslational glycosylation/decoration of CD44v6 with sLe^a. Thus GM35 appears to mediate its functional effects on PMN TEM through engagement of the glycan sLe^a specifically when this glycoepitope is present on the epithelial protein CD44v6.

sLe^a co-localizes apically with CD44v6 and is up-regulated in UC

Further demonstration of the role of sLe^a decorated CD44v6 in regulating PMN detachment from the apical epithelial surface was assessed through comparison of the cellular localization of sLe^a relative to its structural isomer sLe^x and the glycoprotein CD44v6. Confocal microscopic analysis of immunofluorescently stained, non-permeabilized T84 IEC monolayers revealed that GM35 binds specifically to sLe^a on apically expressed CD44v6 (Fig. 6A). Furthermore, immunofluorescence and immunohistochemical analyses of colonic mucosa from individuals with UC reveal increased expression of sLe^a in inflamed tissue versus non-involved regions from the same patient (Fig. 6B,C), indicating that the expression of sLe^a on intestinal epithelial CD44v6 is physiologically relevant to human intestinal inflammation. Furthermore, immunohistochemical analysis of colonic tissue from individuals with UC revealed GM35 staining of material accumulated within the intestinal crypt, consistent our in vitro results indicating PMN-dependent shedding of sLe^a-containing CD44v6 during PMN TEM (Fig. 6C, red arrow). In addition, co-staining of inflamed UC colonic tissue for CD44v6 and sLe^a revealed strong co-localization of these molecules (Fig. 6D), demonstrating the localization of the sLe^a glycan to apically expressed epithelial CD44v6 in inflamed human mucosa.

Intraluminal GM35 attenuates both PMN TEM and associated barrier compromise in murine small intestine

Having previously demonstrated a role for GM35 in the prevention of PMN TEM in vitro, we sought to determine whether these findings could be extended into a murine in vivo model of intestinal inflammation. Epithelial cell preparations from small and large intestine of adult C57BL/6J mice were found to express a glycoprotein recognized by western blot by GM35 (Fig. 7A). Furthermore, this glycoprotein was of comparable molecular weight to mouse CD44v6 (~200kD). However, in contrast to human tissues, there was robust basal expression of both CD44v6 and the GM35 epitope in murine small and large intestinal epithelium in the absence of exogenous inflammatory stimuli (Fig. 6B,C).

The presence of a GM35-binding glycoprotein in murine intestine supported further investigations of the physiologic relevance of the functional effects of GM35 in mouse intestine. Initially, it was verified that injection of exogenous chemoattractant into a closed externalized loop of small intestine from an anesthetized mouse would, within 60 minutes, result in quantifiable migration of PMNs into the intestinal lumen (model in Fig. 7B, Fig. 7C). In the absence of exogenous chemoattractant, PMN were not detected within the

intestinal lumen. However, injection of either fMLF (100μM) or the murine cytokine KC, resulted in a significant influx of PMN. Importantly, co-injection of GM35 along with fMLF resulted in a significant decrease in the number of PMN reaching the intestinal lumen, relative to those treated with fMLF and an isotype control mAb (Fig. 7C).

It has previously been shown that PMN infiltration into intestinal tissues disrupts intestinal barrier function (48). Therefore we examined whether GM35-dependent blockade of PMN TEM would alter barrier function in this model. Isolated small intestinal loops were injected intraluminally with fMLF, in the presence of either GM35 or an isotype-matched IgG control mAb, and PMN migration was allowed to proceed for 60 minutes. These same loops were then injected with 10kDa FITC-conjugated dextran and incubated for an additional 30 minutes. At this time, mice were sacrificed and intestinal permeability was quantified by measurement of fluorescence of the peripheral blood. PMN migration into the intestinal lumen was indeed accompanied by increased intestinal permeability to 10kD FITC dextran (Fig. 7D). Furthermore, this increase in permeability was prevented by either mAb GM35 or by systemic neutrophil depletion, using an antiLy6G mAb (200μg, I.P., 24 hours prior to the experiment) (Fig. 7D). Thus, luminal GM35 blocked both chemoattractant stimulated PMN TEM and associated increases in permeability in murine small intestine.

Discussion

Controlled PMN TEM is an essential component of the innate immune response against invading microorganisms. However, dysregulated influx of PMNs across the intestinal epithelium results in the formation of crypt abscesses and is indicative of IBD. PMN accumulation at epithelial surfaces is also relevant to other inflammatory processes including periodontitis, cystitis, and infectious enterocolitis (49). Therefore, a greater understanding of the mechanisms governing the late stages of PMN TEM, including PMN detachment from the apical epithelium may provide new and unique therapeutic targets for regulating mucosal inflammation. Using the unique mAb GM35 we have recently demonstrated that shedding of the extracellular domain of CD44v6 is associated with PMN detachment from the apical epithelial surface. Here, we extend these findings to identify a novel role for the sialylated glycan sLe^a displayed by the epithelial protein CD44v6 in the regulation of the interaction between migrating PMN and the apical aspect of the intestinal epithelium.

Immunoblotting and mass spectrometric analyses revealed that sLe^a on CD44v6 is exclusively O-linked and independent of N-glycosylation. These results are consistent with evidence that most variant exons of CD44, including CD44v6 are primarily O-glycosylated (13, 50, 51), with only two alternative exons (CD44v5 and CD44v10) containing NXS/T, the motif for N-glycosylation (13). Furthermore, many of the O-glycans attached to CD44 variant glycoproteins terminate with sialic acid residues (50), consistent with the results of the current study revealing that the sialic acid is essential for GM35 ligand binding.

Expansion of these findings using glycan array analysis technology identified the highest affinity glycotope recognized by GM35 as the sialic acid-containing glycan determinant sLe^a. Lower affinity binding to sLe^c, the non-fucosylated biosynthetic precursor of sLe^a,

was also detected. However, sLe^c localized exclusively to N-linked glycans at the apical surface of T84 IECs, and a mAb to anti-sLe^c (Dupan-2) had no functional effect on PMN TEM. Furthermore, expression of sLe^c has been previously been associated primarily with the large transmembrane glycoprotein Muc-1 (52, 53) and not with CD44v6.

The glycans of glycoproteins, including CD44, are known to serve as ligands in recognition systems particularly in inflammation and immunity (54, 55), and glycans displayed by cell surface glycoproteins have been shown to play an important role in the regulation of leukocyte trafficking (56). Interestingly leukocyte expressed N-linked glycans are known to act as ligands for E-selectin. Additionally, neutrophil core-1-derived O-glycans can also function to bind E-selectin (57). Furthermore, loss of intestinal epithelial cell-specific core 1-derived O-glycans is associated with spontaneous colitis in mice (58). Here, we identify a novel role for a sLe^a-containing core 2 glycan in PMN-epithelial interactions in the intestine.

In further support of a role for sLe^a in modulating events at the apical epithelial surface of the intestine during inflammation, this tetrasaccharide determinant, first described by Koprowski *et al* (38), has been previously been reported to be highly expressed on the surface of established human pancreatic, colon and gastric cancer cell lines, in vitro *(59, 60)* as well as in human adenocarcinomas of the colon, stomach, gall-bladder and pancreas (38, 61, 62). While sLe^a itself has previously been reported to act as an important mediator of cell-cell adhesion (63), the current studies of PMN TEM represent the first report of a role for this carbohydrate antigen in the regulation of PMN trafficking. Specifically we demonstrate that sLe^a on CD44v6 can be targeted to significantly inhibit PMN TEM through inhibition of cleavage of CD44v6 and the detachment of PMN from the luminal epithelial surface. These findings identify a novel, glycan-dependent mechanism for the regulation of PMN TEM and provide the first evidence of a functional role for sLe^a in mucosal inflammation.

We discovered in our study, an epithelial cell-specific expression pattern for sLe^a, with robust expression observed in T84 and HT29 but not Caco2 or SKCO15 IECs. This restricted pattern of expression for sLe^a was further confirmed by mass spectrometric mapping of the surface glycans expressed by each of the IEC lines examined in the current study. This cell specific expression pattern for sLe^a was exploited in order to identify specific glycosyltransferases involved in the biosynthesis of sLe^a in human IECs. Comparative analysis of galactosyl, sialyl and fucosyl transferase expression in sLe^a expressing (T84 and HT29), and sLe^a non-expressing (Caco2 and SKCO15) IECs demonstrated numerous differences relevant to the biosynthesis of this inflammation-responsive sLe^a determinant.

Most significantly, expression levels of the fucosyltransferases revealed a profound increase in the expression of α3/4-Fut3 in T84 IECs relative to SKCO15 and Caco2 IECs. The absence of α3/4-Fut3 in SKCO15 IECs correlates with the lack of expression of fucosylated Lewis structures observed by mass spectrometric characterization of the SKCO15 glycan profile. In support of the role of Fut3 in the generation of the GM35 antigen sLe^a in human IECs, Fut3 predominantly exhibits α1-4 fucosyltransferase activity and has previously been implicated in the synthesis of sLe^a in other systems (46, 47). Further it has also been

previously reported that α1-3 fucosyltransferases catalyze the final step in the synthesis of a range of glycoconjugates know to be involved in cell adhesion and lymphocyte recirculation (47). Thus, differing levels of sLe^a synthesis are likely to be due, in part, to the massive differences in Fut3 expression seen across IECs. In support of this, transfection of Fut3 into SKCO15 IECs induced a robust expression of the sLe^a glycoepitope. However, despite successful forced expression of sLe^a in these Fut3 expressing SKCO15 cells, GM35 did not block PMN TEM across these transfected IECs. This lack of a functional effect of GM35 in these sLe^a expressing SKCO15 IECs was attributed to the observation that though these cells synthesized sLe^a, this glycoepitope was not displayed on CD44v6, further underscoring the importance of the role of this epithelial glycoprotein in regulating PMN TEM.

The current findings also emphasize the physiologic relevance of sLe^a on CD44v6 to intestinal inflammation. sLe^a is upregulated in concert with CD44v6 in inflamed regions of human colon from patients with UC. Furthermore, luminal injection of GM35 blocks PMN TEM in vivo. This blockade of PMN TEM is associated with preservation of intestinal barrier function, normally compromised by PMN TEM. Therefore it is highly likely that future identification of both the specific GM35 binding glycan determinant (either sLe^a or sLe^c), and the associated protein ligand in murine intestinal tissues, as well as further characterization of the novel glycan profile of normal and inflamed murine intestinal epithelium, will provide useful targets for future therapeutics in IBD. Given that expression of both CD44v6 (12) and the sLe^a determinant are upregulated in the intestinal crypts of patients with ulcerative colitis, this novel glycosylation-dependent interaction is a promising potential target for therapeutic intervention in IBD.

Supplementary Material

Refer to Web version on PubMed Central for supplementary material.

Acknowledgments

We would like to thank Dr. Miao and Rong Jiang, MD from the department of Human genetics at Emory University for their help with MS/MS analysis. We would like to thank Tony Liang for his assistance with design of initial deglycosylation experiments. We would also like to thank Dr. Maria Delgado and Dr. Brad Farris from the department of Pathology and Laboratory Medicine, Emory University for their expert help with the IHC staining of human intestinal mucosa samples.

This work was supported by funding from National Institutes of Health Grants DK079392 and DK072564 (64), R01DK089763 and R01DK055679 (AN), R24GM098791 and U01CA168930 (RDC) and U54GM062116 (Consortium for Functional Glycomics), as well as a seed grant from the Emory University Research Council (NAL), and Career Development (JCB) and Senior Research Awards from the Crohn's & Colitis Foundation of America (NAL).

Abbreviations in this paper include

Benzyl-Gal-NAc	2-acetamido-2-deoxy-α-D-galactopyranoside
CD44v6	CD44 variant containing exon 6
CFG	Consortium for Functional Genomics
ECD	Extracellular domain

Fuc	Fucose
Fut3	α3/4 Fucosyltransferase 3
Fut6	α1/3 Fucosyltransferase 6
Gal	Galactose
GlcNAc	N-acetylglucosamine
IBD	Inflammatory bowel disease
IECs	Intestinal epithelial cells
Neu5Ac	N-acetylneuraminic acid
PMN	Polymorphonuclear leukocyte
sLe^a	Sialyl Lewis A
sLe^c	Sialyl Lewis C
sLe^x	Sialyl Lewis X
St3Gal3	α2/3 sialyltransferase 3
TEM	Transepithelial migration
UC	Ulcerative Colitis

References

1. Xavier RJ, Podolsky DK. Unravelling the pathogenesis of inflammatory bowel disease. Nature. 2007; 448:427–434. [PubMed: 17653185]
2. Brazil JC, Louis NA, Parkos CA. The Role of Polymorphonuclear Leukocyte Trafficking in the Perpetuation of Inflammation During Inflammatory Bowel Disease. Inflamm Bowel Dis. 2013
3. Woodfin A, Voisin MB, Imhof BA, Dejana E, Engelhardt B, Nourshargh S. Endothelial cell activation leads to neutrophil transmigration as supported by the sequential roles of ICAM-2, JAM-A, and PECAM-1. Blood. 2009; 113:6246–6257. [PubMed: 19211506]
4. Ley K, Laudanna C, Cybulsky MI, Nourshargh S. Getting to the site of inflammation: the leukocyte adhesion cascade updated. Nat Rev Immunol. 2007; 7:678–689. [PubMed: 17717539]
5. Imhof BA, Dunon D. Basic mechanism of leukocyte migration. Horm Metab Res. 1997; 29:614–621. [PubMed: 9497898]
6. Blake KM, Carrigan SO, Issekutz AC, Stadnyk AW. Neutrophils migrate across intestinal epithelium using beta2 integrin (CD11b/CD18)-independent mechanisms. Clin Exp Immunol. 2004; 136:262–268. [PubMed: 15086389]
7. Liu Y, Buhring HJ, Zen K, Burst SL, Schnell FJ, Williams IR, Parkos CA. Signal regulatory protein (SIRPalpha), a cellular ligand for CD47, regulates neutrophil transmigration. J Biol Chem. 2002; 277:10028–10036. [PubMed: 11792697]
8. Parkos CA, Colgan SP, Diamond MS, Nusrat A, Liang TW, Springer TA, Madara JL. Expression and polarization of intercellular adhesion molecule-1 on human intestinal epithelia: consequences for CD11b/CD18-mediated interactions with neutrophils. Mol Med. 1996; 2:489–505. [PubMed: 8827719]
9. Parkos CA, Colgan SP, Liang TW, Nusrat A, Bacarra AE, Carnes DK, Madara JL. CD47 mediates post-adhesive events required for neutrophil migration across polarized intestinal epithelia. J Cell Biol. 1996; 132:437–450. [PubMed: 8636220]

10. Reaves TA, Colgan SP, Selvaraj P, Pochet MM, Walsh S, Nusrat A, Liang TW, Madara JL, Parkos CA. Neutrophil transepithelial migration: regulation at the apical epithelial surface by Fc-mediated events. Am J Physiol Gastrointest Liver Physiol. 2001; 280:G746–754. [PubMed: 11254502]
11. Zen K, Liu DQ, Li LM, Chen CX, Guo YL, Ha B, Chen X, Zhang CY, Liu Y. The heparan sulfate proteoglycan form of epithelial CD44v3 serves as a CD11b/CD18 counter-receptor during polymorphonuclear leukocyte transepithelial migration. J Biol Chem. 2009; 284:3768–3776. [PubMed: 19073595]
12. Brazil JC, Lee WY, Kolegraff KN, Nusrat A, Parkos CA, Louis NA. Neutrophil migration across intestinal epithelium: evidence for a role of CD44 in regulating detachment of migrating cells from the luminal surface. J Immunol. 2010; 185:7026–7036. [PubMed: 20974992]
13. Screaton GR, Bell MV, Jackson DG, Cornelis FB, Gerth U, Bell JI. Genomic structure of DNA encoding the lymphocyte homing receptor CD44 reveals at least 12 alternatively spliced exons. Proc Natl Acad Sci U S A. 1992; 89:12160–12164. [PubMed: 1465456]
14. St John T, Meyer J, Idzerda R, Gallatin WM. Expression of CD44 confers a new adhesive phenotype on transfected cells. Cell. 1990; 60:45–52. [PubMed: 2403843]
15. Thomas L, Byers HR, Vink J, Stamenkovic I. CD44H regulates tumor cell migration on hyaluronate-coated substrate. J Cell Biol. 1992; 118:971–977. [PubMed: 1380003]
16. Aruffo A, Stamenkovic I, Melnick M, Underhill CB, Seed B. CD44 is the principal cell surface receptor for hyaluronate. Cell. 1990; 61:1303–1313. [PubMed: 1694723]
17. Okamoto I, Kawano Y, Tsuiki H, Sasaki J, Nakao M, Matsumoto M, Suga M, Ando M, Nakajima M, Saya H. CD44 cleavage induced by a membrane-associated metalloprotease plays a critical role in tumor cell migration. Oncogene. 1999; 18:1435–1446. [PubMed: 10050880]
18. Herrlich P, Sleeman J, Wainwright D, Konig H, Sherman L, Hilberg F, Ponta H. How tumor cells make use of CD44. Cell Adhes Commun. 1998; 6:141–147. [PubMed: 9823465]
19. Gunthert U, Hofmann M, Rudy W, Reber S, Zoller M, Haussmann I, Matzku S, Wenzel A, Ponta H, Herrlich P. A new variant of glycoprotein CD44 confers metastatic potential to rat carcinoma cells. Cell. 1991; 65:13–24. [PubMed: 1707342]
20. Johnson P, Maiti A, Brown KL, Li R. A role for the cell adhesion molecule CD44 and sulfation in leukocyte-endothelial cell adhesion during an inflammatory response? Biochem Pharmacol. 2000; 59:455–465. [PubMed: 10660111]
21. Ponta H, Sherman L, Herrlich PA. CD44: from adhesion molecules to signalling regulators. Nat Rev Mol Cell Biol. 2003; 4:33–45. [PubMed: 12511867]
22. Tolg C, Hofmann M, Herrlich P, Ponta H. Splicing choice from ten variant exons establishes CD44 variability. Nucleic Acids Res. 1993; 21:1225–1229. [PubMed: 8464707]
23. Brown TA, Bouchard T, St John T, Wayner E, Carter WG. Human keratinocytes express a new CD44 core protein (CD44E) as a heparan-sulfate intrinsic membrane proteoglycan with additional exons. J Cell Biol. 1991; 113:207–221. [PubMed: 2007624]
24. Jalkanen S, Jalkanen M. Lymphocyte CD44 binds the COOH-terminal heparin-binding domain of fibronectin. J Cell Biol. 1992; 116:817–825. [PubMed: 1730778]
25. Parkos CA, Delp C, Arnaout MA, Madara JL. Neutrophil migration across a cultured intestinal epithelium. Dependence on a CD11b/CD18-mediated event and enhanced efficiency in physiological direction. J Clin Invest. 1991; 88:1605–1612. [PubMed: 1682344]
26. Liu Y, Merlin D, Burst SL, Pochet M, Madara JL, Parkos CA. The role of CD47 in neutrophil transmigration. Increased rate of migration correlates with increased cell surface expression of CD47. J Biol Chem. 2001; 276:40156–40166. [PubMed: 11479293]
27. Mandell KJ, McCall IC, Parkos CA. Involvement of the junctional adhesion molecule-1 (JAM1) homodimer interface in regulation of epithelial barrier function. J Biol Chem. 2004; 279:16254–16262. [PubMed: 14749337]
28. Balsam LB, Liang TW, Parkos CA. Functional mapping of CD11b/CD18 epitopes important in neutrophil-epithelial interactions: a central role of the I domain. J Immunol. 1998; 160:5058–5065. [PubMed: 9590256]
29. Mackarel AJ, Russell KJ, Ryan CM, Hislip SJ, Rendall JC, FitzGerald MX, O'Connor CM. CD18 dependency of transendothelial neutrophil migration differs during acute pulmonary inflammation. J Immunol. 2001; 167:2839–2846. [PubMed: 11509630]

30. Colgan SP, Parkos CA, McGuirk D, Brady HR, Papayianni AA, Frendl G, Madara JL. Receptors involved in carbohydrate binding modulate intestinal epithelial-neutrophil interactions. J Biol Chem. 1995; 270:10531–10539. [PubMed: 7537733]

31. Colgan SP, Parkos CA, Delp C, Arnaout MA, Madara JL. Neutrophil migration across cultured intestinal epithelial monolayers is modulated by epithelial exposure to IFN-gamma in a highly polarized fashion. J Cell Biol. 1993; 120:785–798. [PubMed: 8093887]

32. Karhausen J, Furuta GT, Tomaszewski JE, Johnson RS, Colgan SP, Haase VH. Epithelial hypoxia-inducible factor-1 is protective in murine experimental colitis. J Clin Invest. 2004; 114:1098–1106. [PubMed: 15489957]

33. Schnoor M, Cullen P, Lorkowski J, Stolle K, Robenek H, Troyer D, Rauterberg J, Lorkowski S. Production of type VI collagen by human macrophages: a new dimension in macrophage functional heterogeneity. J Immunol. 2008; 180:5707–5719. [PubMed: 18390756]

34. Daley JM, Thomay AA, Connolly MD, Reichner JS, Albina JE. Use of Ly6G-specific monoclonal antibody to deplete neutrophils in mice. J Leukoc Biol. 2008; 83:64–70. [PubMed: 17884993]

35. Brockhausen I, Schachter H, Stanley P. O-GalNAc Glycans. 2009

36. Inoue S, Sato C, Kitajima K. Extensive enrichment of N-glycolylneuraminic acid in extracellular sialoglycoproteins abundantly synthesized and secreted by human cancer cells. Glycobiology. 2010; 20:752–762. [PubMed: 20197272]

37. Peracaula R, Royle L, Tabares G, Mallorqui-Fernandez G, Barrabes S, Harvey DJ, Dwek RA, Rudd PM, de Llorens R. Glycosylation of human pancreatic ribonuclease: differences between normal and tumor states. Glycobiology. 2003; 13:227–244. [PubMed: 12626415]

38. Koprowski H, Steplewski Z, Mitchell K, Herlyn M, Herlyn D, Fuhrer P. Colorectal carcinoma antigens detected by hybridoma antibodies. Somatic Cell Genet. 1979; 5:957–971. [PubMed: 94699]

39. Reis CA, Osorio H, Silva L, Gomes C, David L. Alterations in glycosylation as biomarkers for cancer detection. J Clin Pathol. 2010; 63:322–329. [PubMed: 20354203]

40. Cao H, Crocker PR. Evolution of CD33-related siglecs: regulating host immune functions and escaping pathogen exploitation? Immunology. 2011; 132:18–26. [PubMed: 21070233]

41. von Gunten S, Yousefi S, Seitz M, Jakob SM, Schaffner T, Seger R, Takala J, Villiger PM, Simon HU. Siglec-9 transduces apoptotic and nonapoptotic death signals into neutrophils depending on the proinflammatory cytokine environment. Blood. 2005; 106:1423–1431. [PubMed: 15827126]

42. Erickson-Miller CL, Freeman SD, Hopson CB, D'Alessio KJ, Fischer EI, Kikly KK, Abrahamson JA, Holmes SD, King AG. Characterization of Siglec-5 (CD170) expression and functional activity of anti-Siglec-5 antibodies on human phagocytes. Exp Hematol. 2003; 31:382–388. [PubMed: 12763136]

43. Singh R, Subramanian S, Rhodes JM, Campbell BJ. Peanut lectin stimulates proliferation of colon cancer cells by interaction with glycosylated CD44v6 isoforms and consequential activation of c-Met and MAPK: functional implications for disease-associated glycosylation changes. Glycobiology. 2006; 16:594–601. [PubMed: 16571666]

44. Gassmann P, Kang ML, Mees ST, Haier J. In vivo tumor cell adhesion in the pulmonary microvasculature is exclusively mediated by tumor cell--endothelial cell interaction. BMC Cancer. 2010; 10:177. [PubMed: 20433713]

45. Kakiuchi Y, Tsuji S, Tsujii M, Murata H, Kawai N, Yasumaru M, Kimura A, Komori M, Irie T, Miyoshi E, Sasaki Y, Hayashi N, Kawano S, Hori M. Cyclooxygenase-2 activity altered the cell-surface carbohydrate antigens on colon cancer cells and enhanced liver metastasis. Cancer Res. 2002; 62:1567–1572. [PubMed: 11888937]

46. Carvalho AS, Harduin-Lepers A, Magalhaes A, Machado E, Mendes N, Costa LT, Matthiesen R, Almeida R, Costa J, Reis CA. Differential expression of alpha-2,3-sialyltransferases and alpha-1,3/4-fucosyltransferases regulates the levels of sialyl Lewis a and sialyl Lewis x in gastrointestinal carcinoma cells. Int J Biochem Cell Biol. 2010; 42:80–89. [PubMed: 19781661]

47. de Vries T, Knegtel RM, Holmes EH, Macher BA. Fucosyltransferases: structure/function studies. Glycobiology. 2001; 11:119R–128R.

48. Madara JL. Migration of neutrophils through epithelial monolayers. Trends Cell Biol. 1994; 4:4–7. [PubMed: 14731822]

49. Jaye DL, Parkos CA. Neutrophil migration across intestinal epithelium. Ann N Y Acad Sci. 2000; 915:151–161. [PubMed: 11193572]
50. Jackson DG, Bell JI, Dickinson R, Timans J, Shields J, Whittle N. Proteoglycan forms of the lymphocyte homing receptor CD44 are alternatively spliced variants containing the v3 exon. J Cell Biol. 1995; 128:673–685. [PubMed: 7532175]
51. Lokeshwar VB, Bourguignon LYW. Posttranslational Protein Modification and Expression of Ankyrin-Binding Site(S) in Gp85 (Pgp-1/Cd44) and Its Biosynthetic Precursors during T-Lymphoma Membrane Biosynthesis. Journal of Biological Chemistry. 1991; 266:17983–17989. [PubMed: 1833390]
52. Aubert M, Panicot L, Crotte C, Gibier P, Lombardo D, Sadoulet MO, Mas E. Restoration of alpha(1,2) fucosyltransferase activity decreases adhesive and metastatic properties of human pancreatic cancer cells. Cancer Res. 2000; 60:1449–1456. [PubMed: 10728712]
53. Lan MS, Khorrami A, Kaufman B, Metzgar RS. Molecular characterization of a mucin-type antigen associated with human pancreatic cancer. The DU-PAN-2 antigen. J Biol Chem. 1987; 262:12863–12870. [PubMed: 2442170]
54. McEver RP. Selectin-carbohydrate interactions during inflammation and metastasis. Glycoconj J. 1997; 14:585–591. [PubMed: 9298691]
55. Crocker PR, Feizi T. Carbohydrate recognition systems: functional triads in cell-cell interactions. Curr Opin Struct Biol. 1996; 6:679–691. [PubMed: 8913692]
56. Sperandio M, Gleissner CA, Ley K. Glycosylation in immune cell trafficking. Immunol Rev. 2009; 230:97–113. [PubMed: 19594631]
57. Yago T, Fu J, McDaniel JM, Miner JJ, McEver RP, Xia L. Core 1-derived O-glycans are essential E-selectin ligands on neutrophils. Proc Natl Acad Sci U S A. 2010; 107:9204–9209. [PubMed: 20439727]
58. Fu J, Wei B, Wen T, Johansson ME, Liu X, Bradford E, Thomsson KA, McGee S, Mansour L, Tong M, McDaniel JM, Sferra TJ, Turner JR, Chen H, Hansson GC, Braun J, Xia L. Loss of intestinal core 1-derived O-glycans causes spontaneous colitis in mice. J Clin Invest. 2011; 121:1657–1666. [PubMed: 21383503]
59. Falk KE, Karlsson KA, Larson G, Thurin J, Blaszczyk M, Steplewski Z, Koprowski H. Mass spectrometry of a human tumor glycolipid antigen being defined by mouse monoclonal antibody NS-19-9. Biochem Biophys Res Commun. 1983; 110:383–391. [PubMed: 6188455]
60. Magnani JL, Nilsson B, Brockhaus M, Zopf D, Steplewski Z, Koprowski H, Ginsburg V. A monoclonal antibody-defined antigen associated with gastrointestinal cancer is a ganglioside containing sialylated lacto-N-fucopentaose II. J Biol Chem. 1982; 257:14365–14369. [PubMed: 7142214]
61. Atkinson BF, Ernst CS, Herlyn M, Steplewski Z, Sears HF, Koprowski H. Gastrointestinal cancer-associated antigen in immunoperoxidase assay. Cancer Res. 1982; 42:4820–4823. [PubMed: 6751528]
62. Sakamoto S, Watanabe T, Tokumaru T, Takagi H, Nakazato H, Lloyd KO. Expression of Lewisa, Lewisb, Lewisx, Lewisy, siayl-Lewisa, and sialyl-Lewisx blood group antigens in human gastric carcinoma and in normal gastric tissue. Cancer Res. 1989; 49:745–752. [PubMed: 2910493]
63. Takada A, Ohmori K, Yoneda T, Tsuyuoka K, Hasegawa A, Kiso M, Kannagi R. Contribution of carbohydrate antigens sialyl Lewis A and sialyl Lewis X to adhesion of human cancer cells to vascular endothelium. Cancer Res. 1993; 53:354–361. [PubMed: 7678075]
64. Chiaravalli AM, Cornaggia M, Furlan D, Capella C, Fiocca R, Tagliabue G, Klersy C, Solcia E. The role of histological investigation in prognostic evaluation of advanced gastric cancer. Analysis of histological structure and molecular changes compared with invasive pattern and stage. Virchows Arch. 2001; 439:158–169. [PubMed: 11561756]

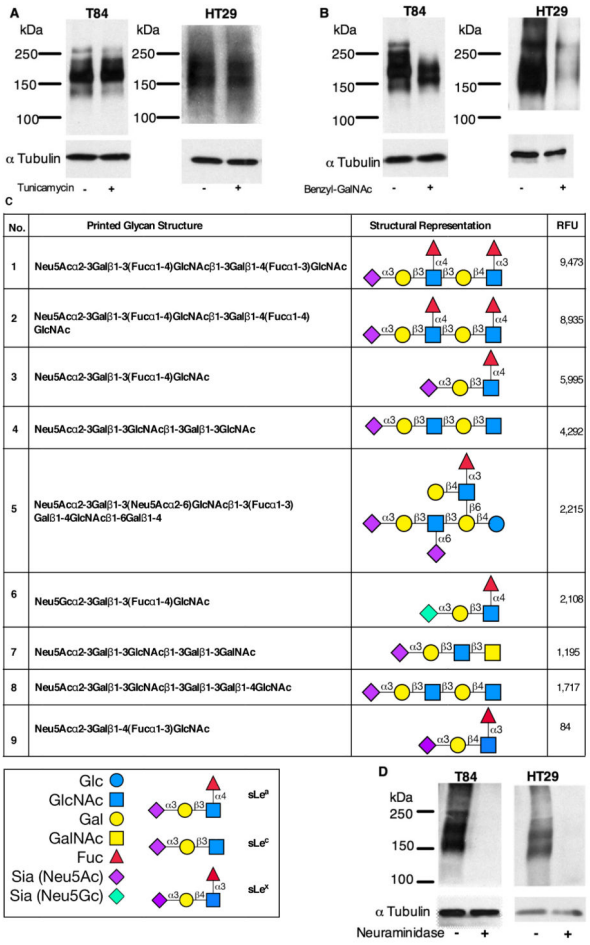

Figure 1. GM35 binds to the O-linked glycan sLe^a

T84 or HT29 IECs were pretreated with (A) 5μg/ml Tunicamycin or (B) 4mM Benzyl-GalNAc before whole cell lysis and western blotting with GM35. Data represent N=3 immunoblots. (C) The glycans recognized by GM35, including glycan number, glycan structure, glycan name and relative fluorescence units (RFU) intensity are depicted with sLe^x is included as a negative binding control. (D) Protein lysates from T84 or HT29 IECs were treated with 50U neuraminidase before whole cell lysis and western blotting with GM35. Data represent N=3 immunoblots.

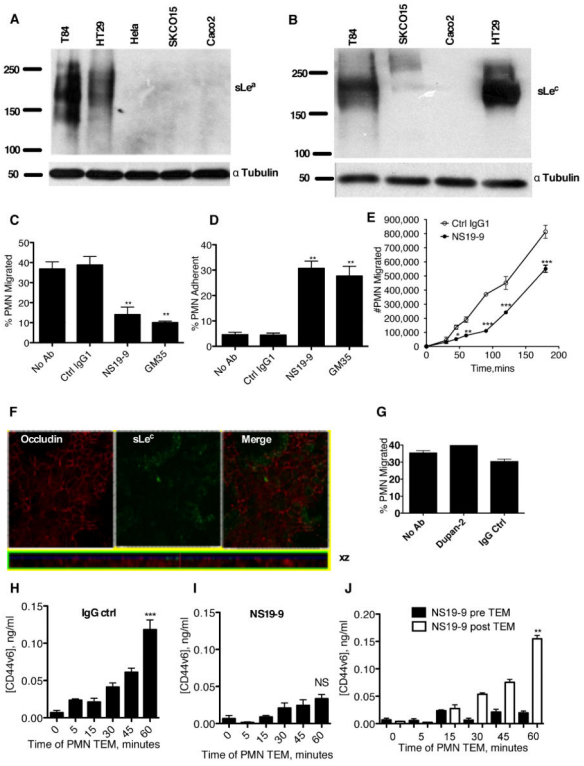

Figure 2. mAb NS19-9 but not Dupan-2 blocks PMN TEM and CD44v6 shedding

Indicated cells were lysed and proteins immunoblotted with NS19-9 (A) or Dupan-2 (B). Confluent T84 monolayers were pre-treated with 10μg/ml NS19-9, 10μg/ml GM35, or 10μg/ml non-inhibitory IgG1 isotype control mAb before 1×10^6 PMNs were added to the basolateral surface. PMNs were allowed to migrate for 1 hour in response to a 100nM gradient of fMLF. The number of migrated PMNs (C) and the number of PMNs which were adherent to the apical epithelial surface (D) were quantified by myeloperoxidase assay. Data depict means ± SE (N=3). (E) Confluent T84 monolayers were treated apically with (closed circle) or without (open circle) 10μg/ml NS 19-9 before the addition of 1×10^6 PMN. PMN transmigration was then measured at the indicated time points. Data are mean +/− SE (n=3). (F) Confluent T84 monolayers were co-stained with 10μg/ml anti-Occludin mAb and 10μg/ml Dupan-2 and analyzed by confocal microscopy. (G) Confluent T84 monolayers were pre-treated with 10μg/ml Dupan-2 or 10μg/ml non-inhibitory IgG isotype control mAb before 1×10^6 PMNs were added to the basolateral surface. PMNs were allowed to migrate for 1 hour in response to a 100nM gradient of fMLF. The numbers of migrated PMN were quantified by myeloperoxidase assay. Data are means ± SE (N=3). 1×10^6 PMNs were added to confluent T84 monolayers treated apically with 10μg/ml binding control IgG1 (H) or 10μg/ml NS19-9 (I). PMNs were allowed to migrate in the basolateral to apical direction in response to a 100nM gradient of fMLF. At the time-points indicated the T84 containing filters were removed, and the solution from the apical migration reservoir assayed for soluble CD44v6 by ELISA. (J) Addition of mAb NS19-9 to the apical migration reservoir following PMN TEM does not prevent binding of released CD44v6 to the capture or detection ELISA mAbs. Significance was defined as $p<0.05$ (*, $p<0.05$; **, $p<0.01$; ***, $p<0.001$).

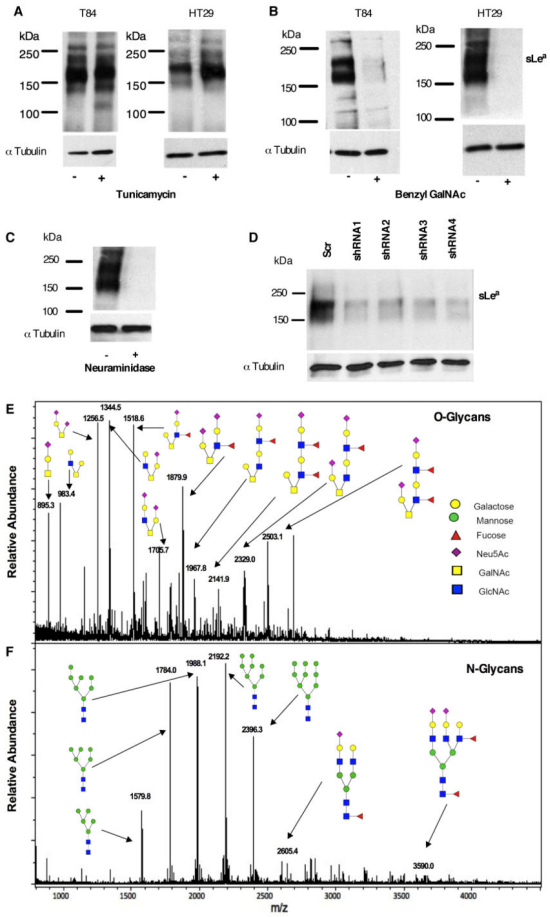

Figure 3. NS19-9 and GM35 bind to O-linked sLe^a

T84 or HT29 IECs were pretreated with (A) 5μg/ml Tunicamycin or (B) 4mM Benzyl-GalNAc before whole cell lysis and western blotting with NS19-9. (C) Protein lysates isolated from T84 IECs were treated with neuraminidase before immunoblotting with NS19-9. (D) Representative immunoblot demonstrating that transfection of HT29 IECs with CD44 gene silencing plasmids (shRNA1-3) decreased the expression of sLe^a detected by NS19-9 as compared to scrambled control. Data depicts representative results from N=3 immunoblots. MALDI-TOF/TOF spectrometric analysis of the O-linked (E), and N-linked (F) derivatized and permethylated glycans isolated from T84 IECs.

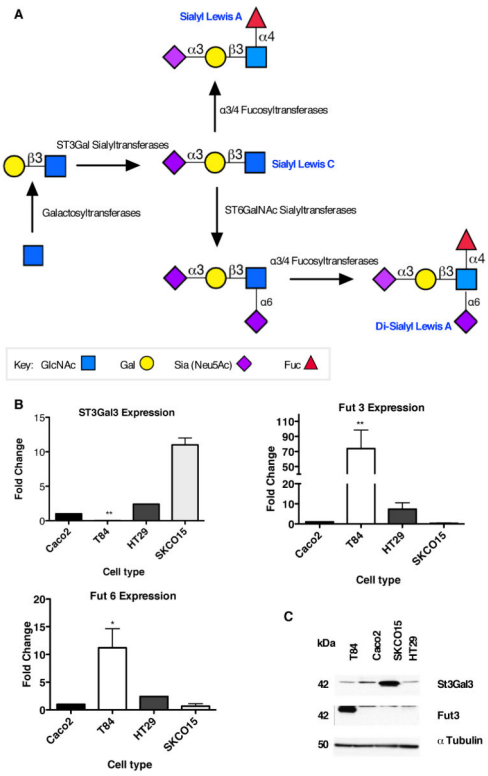

Figure 4. Differential expression of glycosyltransferases in human IECs

(A) Schematic representation of the glycosyltransferases responsible for the biosynthesis of sLe^a. (B) RNA was isolated from indicated IECs and analyzed by real-time PCR for levels of expression of ST3Gal3, Fut3 and Fut6. Results are depicted as fold change relative to Caco2 IECs and normalized for expression of the housekeeping gene GAPDH. N=3-6, significance was defined at $p<0.05$ (*, $p<0.05$; **, $p<0.01$; ***, $p<0.001$). (C) Following epithelial cell lysis, equal amounts of protein lysates from indicted IECs were subjected to SDS-PAGE under reducing conditions and immunoblotted with indicated antibodies. Data represent N=3 immunoblots.

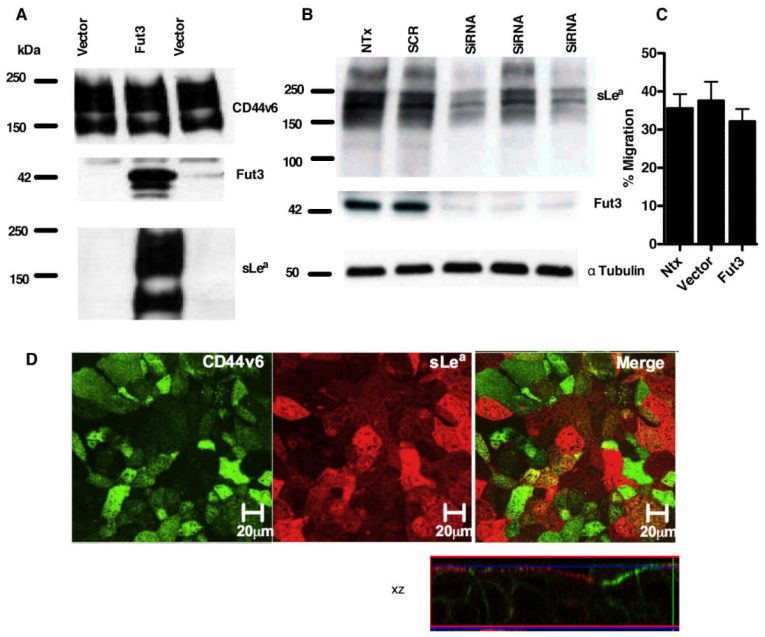

Figure 5. Fut3 drives sLe^a expression in SKCO15 IECs but not on CD44v6

(A) SKCO15 IECs transfected with empty vector or Fut3 containing vector were immunoblotted with indicated antibodies. Data represent N=3 immunoblots. (B) HT29 IECs either non-transfected or transfected with Scr or Fut3 siRNA were lysed and immunoblotted with antibodies against Fut3 and sLe^a. (C) Non-transfected SKCO15 IECs and SKCO15 IECs transfected with Fut3 or an empty vector were grown as confluent inverted monolayers. Monolayers were pre-treated apically with 10μg/ml GM35 mAb before 1×10^6 PMNs were added to the basolateral surface. PMNs were allowed to migrate for 1 hour in response to a 100nM gradient of fMLF. The number of migrated PMNs was quantified by myeloperoxidase assay. (D) Confluent Fut3 transfected/ sLe^a expressing SKCO15 monolayers were co-stained with 10μg/ml GM35 (red) and 10μg/ml anti-CD44v6 mAb (green). Apical protein localization was determined by confocal microscopy analysis. Representative images from N=3 experiments are shown both en face or in the xz plane of section.

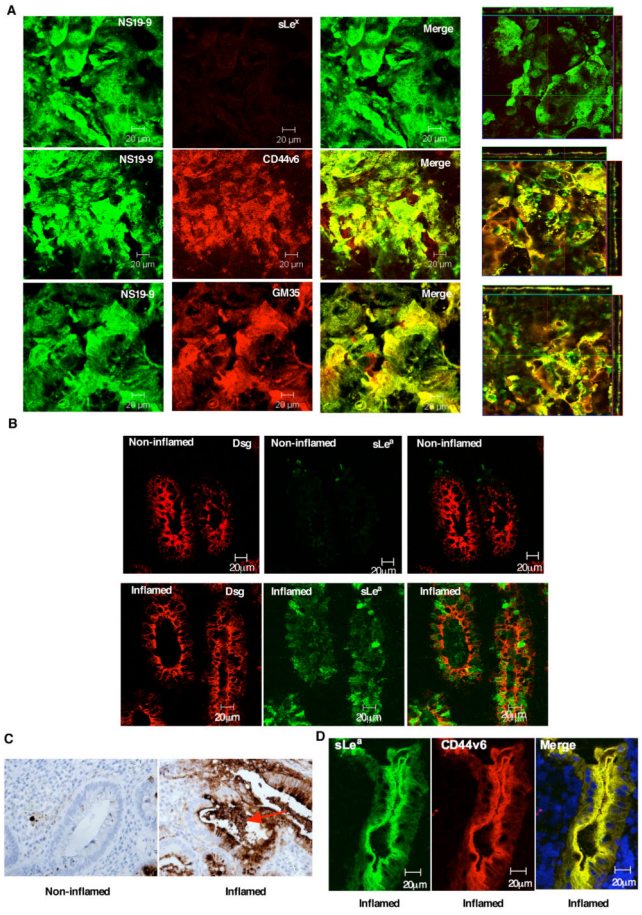

Figure 6. NS19-9 and GM35 bind to apical sLe^a on CD44v6 in inflamed colonic mucosa

Confluent T84 monolayers were co-stained with 10μg/ml NS19-9 (green) and 10μg/ml GM35, 10μg/ml anti-CD44v6 mAb or 10μg/ml anti-sLe^x mAb (red). Apical protein localization was determined by confocal microscopy analysis. Representative images from N=3 experiments are shown both en face or in the xz plane of section (A). Cryosections of non-inflamed colonic mucosa and inflamed sections of colonic mucosa from patients with active UC were examined for localization of sLe^a (NS19-9, green) and the epithelial marker Desmoglein 1 (red) as described in methods (B). (C) Immunohistochemical analysis of colonic epithelia from a patient with UC was performed using the anti-sLe^a mAb GM35 (brown). Non-involved uninflamed epithelium is compared to active inflammation within a crypt abscesses. (D) Cryosections of inflamed colonic mucosa from patients with active UC were examined for co-localization of sLe^a (GM35, green) and CD44v6 (red) as described in methods.

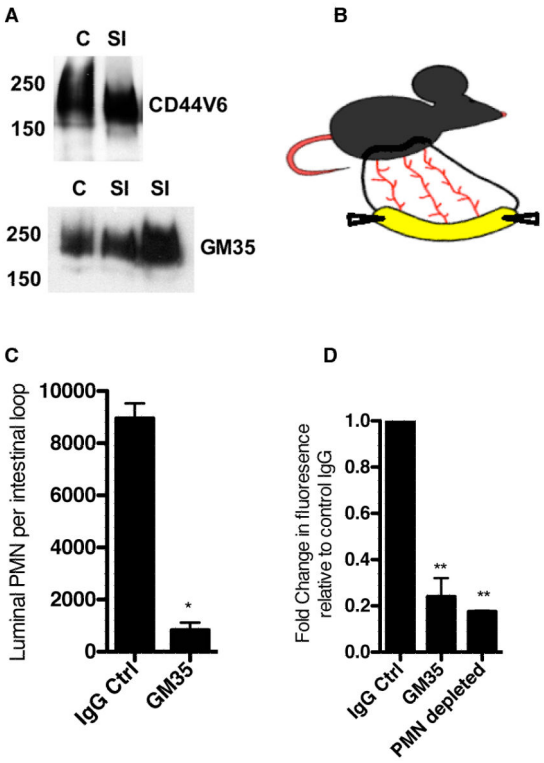

Figure 7. GM35 blocks PMN luminal trafficking *in vivo*

(A) Following epithelial cell isolation from the small intestine and colon of wild type (WT) C57BL/6J mice equal amounts of protein lysates from were subjected to SDS-PAGE under reducing conditions and immunoblotted with indicated antibodies. Data represent N=3 immunoblots. (B) Cartoon demonstrating exteriorization of vascularized small intestinal loop in C57BL/6J mouse. (C) 100μM fMLF along with 50μg GM35 or IgG control mAb was injected into the lumen of a surgically isolated fully vascularized segment of murine small intestine. Following a 90 minute incubation PMN that migrated into the intestinal lumen were quantified by cytospin and Diff-Quik staining. (D) Following sequential injection of 100μM fMLF +/− 50μg indicated mAb and 10kDa FITC dextran into the small intestine of WT C57BL/6J mice with normal PMN levels and mice pretreated with anti-Ly6G mAb to deplete PMN, passage of dextran across the intestinal epithelium was measured by quantification of fluorescence in the peripheral blood. Data are representative of experiments performed on N=3 mice.